Mixing Behavior of Colored Dissolved Organic Matter and Its Potential Ecological Implication in the Caloosahatchee River Estuary, Florida

Zhiqiang Chen · Peter H. Doering · Mayra Ashton · Beth A. Orlando

Abstract Colored dissolved organic matter (CDOM) is one of the most important water quality constituents impacting light attenuation in estuaries; its concentration and distribution influence light quality and quantity available to phytoplankton and submerged aquatic vegetation. By combining field surveys (March 2009–January 2011) and laboratory studies, we examined the estuarine mixing behavior of CDOM and potential loss processes affecting mixing behavior in the Caloosahatchee River Estuary (CRE), Florida. The CDOM absorption coefficient at 355 nm ($a_{CDOM}(355)$, m^{-1}) varied from 0.5 to 64 m^{-1}, with higher values in the upper estuary and lower values downstream, and increased with increasing freshwater inflow. CDOM exhibited three apparent mixing patterns with respect to hypothetical conservative mixing, with (1) conservative behavior or (2) addition at lower inflow and (3) loss at higher inflow. Laboratory studies indicated that flocculation was not a major loss process and that CDOM was susceptible to photolysis. The concentration of CDOM declined as a function of cumulative solar irradiation with a rate of ~0.003 m^2 mol^{-1}, suggesting a photobleaching half-life for CDOM of about 1 w. Apparent nonconservative mixing of CDOM increased or decreased light attenuation by 15–30 %, depending on freshwater inflow and location in the estuary. Light attenuation in the CRE was controlled primarily by CDOM in the upper estuary and by turbidity in the lower estuary, with the average contribution of CDOM to total light attenuation of 55 % (2–92 %) and turbidity of 23 % (3–79 %). The contribution of chlorophyll *a* (Chl *a*) to light attenuation was less than both CDOM and turbidity, accounting for about 12 % on average (2–24 %), regardless of location. These results suggest that any nutrient management scenario aimed at improving water clarity through reduction in Chl *a* concentration should consider the contributions of color and turbidity as well.

Introduction

Colored dissolved organic matter (CDOM, also called color) is the optically active (or colored) fraction of dissolved organic matter (DOM) and is an important contributor to light extinction (McPherson and Miller 1987, 1994; Christian and Sheng 2003). The concentration of CDOM affects light availability needed for primary production by phytoplankton, microalgae, and submerged aquatic vegetation in many estuaries (McPherson et al. 1990; Doering et al. 1994; Corbett and Hale 2006; Chen et al. 2007). More importantly, the concentration of CDOM determines not only the absolute magnitude of light it attenuates but also its contribution to overall light extinction relative to other constituents including chlorophyll *a* (Chl *a*) and turbidity (McPherson and Miller 1987; Christian and Sheng 2003; Kelble et al. 2005). The latter is particularly important because the extent to which Chl *a* controls light attenuation relative to other constituents may influence the success of efforts to enhance water clarity through reductions in nutrient loading and Chl *a* (Greening and Janicki 2006; Greening et al. 2011). Hence, a study of processes that influence the concentration of CDOM, such as apparent estuarine mixing behavior, is of ecological and management significance (Doering et al. 1994; Corbett and Hale 2006).

In many estuaries, CDOM is mostly of terrestrial origin and transported by freshwater inflow (Blough and Del Vecchio

Z. Chen (✉) · P. H. Doering · M. Ashton · B. A. Orlando
South Florida Water Management District, 3301 Gun Club Rd, West Palm Beach, FL 33414, USA
e-mail: zhichen@sfwmd.gov

2002). The mixing of CDOM between river and ocean waters produces a commonly observed inverse relationship between CDOM concentration and salinity as well as a longitudinal gradient in concentration (Branco and Kremer 2005; Bowers and Brett 2008). Mixing often appears conservative because CDOM (1) can be so concentrated in river water that mixing masks photochemical or biological alterations of its concentration and composition and (2) may be mostly refractory and not susceptible to common degradation processes (Rochelle-Newall and Fisher 2002; Kowalczuk et al. 2003). However, CDOM does exhibit nonconservative mixing in some estuaries, and this can vary seasonally (Chen et al. 2007; Del Castillo and Miller 2008). Various processes may account for nonconservative mixing behavior including (1) photolysis and microbial activity (Moran et al. 2000; D'Sa and DiMarco 2009; Shank et al. 2009), (2) flocculation and absorptive removal (Uher et al. 2001), and (3) in situ production by phytoplankton, mangroves, sea grasses, or sediment resuspension events (Boss et al. 2001; Romera-Castillo et al. 2010; Shank et al. 2010). All these processes individually and/or interactively contribute to a complexity of CDOM distribution along the estuarine mixing gradient.

CDOM or color has been monitored in the Caloosahatchee River Estuary for decades (Doering et al. 2006), and its important contribution to light attenuation is well recognized (McPherson and Miller 1987, 1994). However, a systematic study of its mixing behavior and potential impacting factors has been lacking. Particularly, the effect of mixing behavior of CDOM on estimates of light attenuation in the estuary has not been assessed. The objectives of this study were to (1) characterize the estuarine mixing behavior of CDOM in the Caloosahatchee River Estuary (CRE), (2) investigate two processes potentially affecting mixing patterns (specifically flocculation and photolysis), and (3) evaluate the relative contributions of CDOM, turbidity, and Chl a to total light attenuation and how mixing behavior can impact estimates of light attenuation.

Materials and Methods

Study Area

The Caloosahatchee River Estuary (CRE) is located on the southwest coast of Florida. It extends approximately 48 km from the Franklin Lock and Dam (S79) at the head of to San Carlos Bay, where it empties into the Gulf of Mexico (Fig. 1). S79 separates the freshwater river from the estuary and acts, in part, as a salinity barrier. The estuary receives freshwater inflows at S79 derived from Lake Okeechobee and runoff from the watershed upstream of the Franklin Lock and Dam and from runoff from the tidal watershed downstream of S79.

Freshwater Inflow

Daily discharge ($m^3 s^{-1}$) at S79 was downloaded from records kept by the South Florida Water Management District (SFWMD). These daily mean flows were averaged over 21 days prior to the sample dates to represent overall flow conditions associated with each sampling event. Previous studies suggested that the overall flushing time of the CRE was from a few days to more than 60 days, depending on freshwater inflow and location in the estuary (Doering et al. 2006; Wan et al. 2013).

Field Surveys

Fourteen (14) field survey cruises were conducted between March 2009 and January 2011, sampling 12–13 stations along an estuarine salinity gradient extending from the Franklin Lock and Dam (S79 or CES01) to San Carlos Bay Marker 6 (SCBM6) in the Gulf of Mexico (Fig. 1 and Table 1). We applied a phased approach to the study of CDOM in the Caloosahatchee River Estuary. The first four field surveys were devoted primarily to the characterization of CDOM mixing behavior and testing for flocculation in the laboratory. Measurements of the diffuse light attenuation coefficient (k_d) were added to the field survey after September 2009, and laboratory measurements of photolysis were added after December 2009. During the last five surveys (April 2010–January 2011), measurements of turbidity and Chl a were taken along with CDOM to estimate the contribution of these water quality constituents to light attenuation. Water samples were collected at a depth of 0.5 m with a 6.2-L Van Dorn Bottle and transferred into a clean bucket. CDOM or color samples were withdrawn from the bucket with a syringe and then passed manually through a 0.45-μm membrane filter into a 60-ml opaque bottle that was stored on ice until analysis in the laboratory as described below. Chl a samples were also taken from the bucket and stored on ice until processed in the laboratory following the methods described by the Laboratory Standard Operating Procedures (South Florida Water Management District SFWMD 2013). Specifically, water samples were filtered in subdued light through a GF/G glass fiber filter as soon as the samples reached the laboratory. The pigments were extracted with an aqueous acetone solution overnight and measured with Turner AU-10 fluorometer using a narrowed bandwidth of 436 nm (exCitation filter) and 680 nm (emission filter). After collecting the CDOM and Chl a samples, salinity, turbidity, and temperature were measured with a YSI 6600 water quality instrument submerged in the bucket. Before and after each cruise, turbidity probes were calibrated using a two-point calibration as recommended by the manufacturer using 0 NTU (deionized water) and 123 NTU standards (Formazin supplied by YSI). YSI turbidity probes are active sensors with a light emitting diode (LED) as

Fig. 1 Sampling stations in the CRE from Franklin Lock and Dam (S79) to the Gulf of Mexico (subpanel showing the CRE relative to the state of Florida)
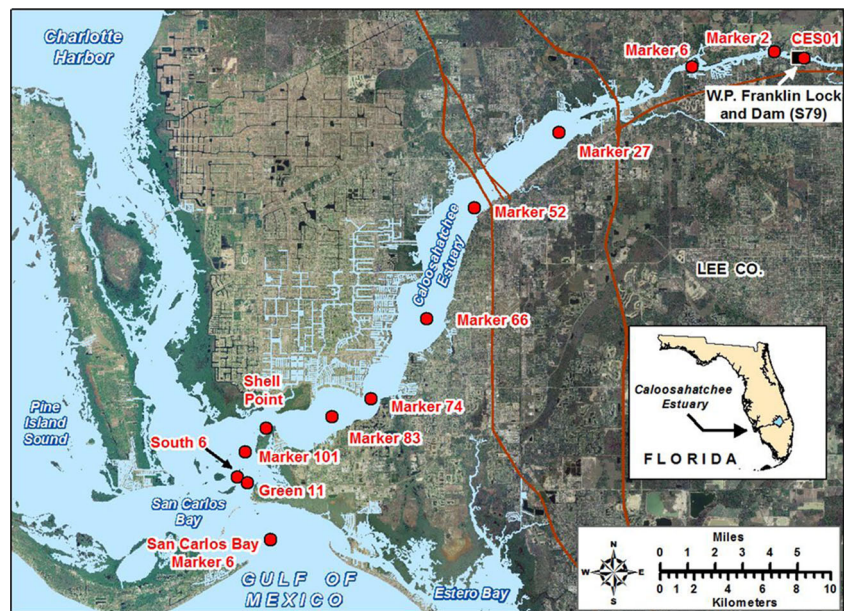
the light source, which produces radiation in the near infrared region of the spectrum. The detection limits of turbidity sensors are from 0 to 100 NTU with a precision of 0.1 NTU and an accuracy of 0.3 NTU or 3 % of readings (whichever is greater). At each of the presumptive end-members of the system (CES01 and SCBM6), a 1-L water sample was collected without filtration and stored on ice for use in laboratory studies.

Vertical profiles of photosynthetically active radiation (PAR) were obtained at depth intervals of 0.25 m with a LI-COR, LI-193 spherical quantum sensor, and a LI-1400 data logger. The diffuse attenuation coefficient (k_d, m^{-1}) of PAR

was calculated from those profiles by curve-fitting using the following equation

$$I_z = I_0 \times \exp(-k_d \times Z) \tag{1}$$

where I_o (µmol sec^{-1} m^{-2}) is PAR just below the water surface and I_z (µmol sec^{-1} m^{-2}) is PAR at depth Z (m). To be consistent among stations of different depths, only data from the top 2 m were used in the calculation.

Table 1 Summary of salinity, CDOM absorption coefficient at 355 (a_{CDOM}(355), m^{-1}), color (PCU), light attenuation coefficient (k_d, m^{-1}) of PAR, photolysis rate (k_p, m^2 mol^{-1}), and CDOM mixing behavior in the field

Dates	Salinity (psu)	a_{CDOM} (355) (m^{-1})	Color (PCU)	k_d (m^{-1})	Mixing behavior	photolysis rate k_p (m^2 mol^{-1})
March 31, 2009	0.1–35.5 (18.5±13.8)	0.5–22.6 (10.6±8.6)	1–49.1 (21.3±18.2)	na	addition (13 %)	na
April 14, 2009	0.33–36.3 (22.2±14.5)	1.0–24.5 (10.6±9.3)	1–41.5 (19.1±15.4)	na	addition (13 %)	na
June 4, 2009	0–36 (16±15)	1.2–38 (15.6±13.3)	11–107 (46±33)	na	loss (-40 %)	na
August 13, 2009	0–25 (7±8)	14–64 (42±17)	41–198 (121±55)	na	loss (-19 %)	na
September 22, 2009	0–31 (8±10)	5–54 (35±16)	23–160 (103±45)	1.03–3.65 (2.17±1.0)	loss(-26 %)	na
December 18, 2009	0–31 (16±11)	4–26 (14±8)	1–50 (22±17)	0.75–1.48 (0.94±0.32)	Conservative (-2 %)	0.004
February 22, 2010	0.3–32 (17±13)	1.6–16.6 (8.9±6.0)	5–38 (21±13)	na	Conservative (-1 %)	0.003
March 23, 2010	0.3–25.5 (7.8±9.2)	5.7–29.3 (18.1±8.6)	19.6–75.4 (45.56±22.6)	0.78–3.36 (1.64±0.84)	loss(-30 %)	0.002
April 19, 2010	0.3–30.9 (11.0±12.5)	2.2–40.2 (23.5±15.2)	6.2–115.0 (64.2±43.1)	0.62–3.48 (1.71±0.94)	loss (-23 %)	0.002
June 14, 2010	0.2–33.0 (11.0±13.3)	2.3–35.2 (21.2±12.7)	8.5–100.2 (56.6±34.6)	0.63–2.26 (1.53±0.52)	loss (-17)	0.002
August 23, 2010	na	na	na	na (only 5 points)	na	0.003
October 25, 2010	0.3–33.8 (16.2±10.9)	3.0–33.9 (18.9±10.7)	12.0–86.6 (48.0±26.2)	0.64–2.48 (1.45±0.64)	Conservative (2 %)	0.002
November 15, 2010	0.3–32.6 (16.9±12.2)	3.8–52.2 (19.8±15.0)	8.3–145.2 (54±42.2)	0.53–1.90 (1.13±0.48)	addition (27 %)	0.003
January 24, 2011	0.4–36.6 (21.1±12.8)	1.5–16.4 (9.7±5.6)	7.2–38.2 (23.5±12.7)	0.74–2.02 (1.25±0.36)	addition (19 %)	0.002

Color was calculated with using a linear regression equation, where Color=a_{CDOM}(465)×16.1+1.4, R^2 =0.997, n=84, p<0.001. Salinity, a_{CDOM}(355), color, and k_d are shown in a format (minimum–maximum (mean±standard deviation)). *na* means not available due to (1) measurements that were not included in those cruises or (2) weather or technical problems

Dilution Experiments for Removal by Flocculation

In the laboratory, samples from freshwater (CES01, FW) and saltwater (SCBM6, SW) end-members were mixed to produce an experimental salinity gradient and mixing curve to test for flocculation. For each survey of 13 sampling events, 11 dilution mixtures were made with the following ratios: 100 mL FW:0 mL SW, 90 mL FW:10 mL SW, 80 mL FW:20 mL SW, 70 mL FW:30 mL SW, 60 mL FW:40 mL SW, 50 mL FW:50 mL SW, 40 mL FW:60 mL SW, 30 mL FW:70 mL SW, 20 mL FW:80 mL SW, 10 mL FW /90 mL SW, and 100 mL SW:0 mL FW. The dilutions were kept at room temperature overnight allowing for interaction between the two end-members. On the following day, samples were filtered for CDOM analysis as described below. The salinity of these dilutions was calculated with the equation (Del Castillo et al. 2000):

$$S_m = S_0 \times \left(1 - \frac{V_f}{V_0 + V_f}\right) + S_f \tag{2}$$

where S_m, S_o, and S_f are salinity (psu) of the dilutions, oceanic, and river end-members, respectively, and V_o and V_f are volumes (mL) of oceanic and river end-members, respectively. Measured CDOM and calculated salinity were examined using salinity–property plots as described below.

Photolysis Experiments

Water samples from the freshwater station (CES01) were filtered first through a 0.45-μm filter to remove particulate matter and then through a 0.2-μm filter to remove most bacteria and placed in autoclaved 150-mL quartz flasks (Ortega-Retuerta et al. 2009). Before each photolysis experiment (total nine experiments), the initial CDOM concentration was measured and treated as concentration at day 0. Five flasks were then placed outdoors under natural sunlight in a water bath along with two additional flasks wrapped thoroughly in aluminum foil to serve as dark controls. Aside from the difference in exposure to light, bottles were subjected to the same experimental conditions. Thus, any differences in CDOM concentration between light and dark bottles were attributed to effects of light. Water temperature ranged from 18 to 32 °C and varied with season. The photolysis experiments lasted for 8 days with CDOM samples taken on days 1, 2, 3, 6, and 8. One flask exposed to light was sacrificed at each time point after day 0, while one of the dark control flasks was sampled repeatedly and the other sacrificed on the last day of the experiment.

The cumulative exposure to PAR (400–700 nm) over the course of each experiment was measured with a LI-COR LI-190 quantum sensor and a LI-1400 data logger. On one occasion, the sensor had a technical problem, and PAR data were obtained from records at a station about 10 mi away from our lab site. The available PAR values from these two stations showed a strong correlation ($R=0.9$, $n=22$).

The CDOM absorption spectra of the control and photolysis samples were measured with the same procedures as field and dilution/flocculation samples. Photolysis rates were estimated using nonlinear fitting of the CDOM absorption coefficient at 355 nm and cumulative PAR (PAR$_{cum}$) data using a first-order decay equation (Shank et al. 2009)

$$a = a_0 \times \exp\left(-k_p \times \text{PAR}_{cum}\right) \tag{3}$$

where a_0 is the initial CDOM absorption coefficient (m^{-1}), a is the CDOM absorption coefficient following exposure to light (m^{-1}), k_p is the photolysis rate (m^2 mol^{-1}) of CDOM, and PAR$_{cum}$ is cumulative solar radiation (mol m^{-2}) over experimental days (8 days).

Measurement of CDOM

The absorption spectra ($A(\lambda)$, dimensionless) of CDOM in the field, dilution, and photolysis samples were measured between 250 and 800 nm at 2-nm intervals using a UV-1601 Shimadzu UV-Visible Spectrophotometer equipped with 1-cm quartz cells. Milli-Q water was used as the blank reference. CDOM absorption coefficients, $a_{CDOM}(\lambda)$ (m^{-1}), were calculated using the following equation (Kirk 1994):

$$a_{CDOM} = 1n10 \times \frac{A(\lambda)}{L} \tag{4}$$

where A is the absorbance, a is the absorption coefficient (m^{-1}), L is the path length (0.01 m), and λ is the wavelength (nm).

The mean absorbance between 700 and 800 nm was subtracted from the spectra to correct for offsets due to instrument baseline drift, temperature, scattering, and other factors (Helms et al. 2008). To determine the extent of photochemical degradation and potential changes in composition of CDOM in the photolysis experiments, three intervals of the spectrum were chosen to derive slopes per Helms et al. (2008): 275–295, 350–400, and 300–700 nm. For the first two intervals, absorbance values were first log-transformed and then linearly fit due to relatively short wavelength intervals. For the third interval, a nonlinear least square regression was used. Previous studies suggested that the ratio (S_R) of the slope at 275–295 nm to the slope at 350–400 nm increases with photochemical degradation, related to the transformation of high molecular weight CDOM (HMW) to low molecular weight CDOM (LMW) (Helms et al. 2008). In addition, we used the absorption coefficient at a wavelength of 355 nm (a(355), m^{-1}) as a measure of CDOM concentration. The absorption coefficient at 465 nm was also calculated and converted to

more commonly used color units (platinum–cobalt unit (PCU)) using a linear regression relationship between $a_{CDOM}(465)$ and color (Color=$a_{CDOM}(465) \times 16.1 + 1.4$, $R^2 = 0.997$, $n = 84$, $p < 0.001$, unpublished data).

Data Analysis

CDOM concentrations measured in the laboratory were plotted against salinity. Apparent mixing behavior in the field was examined by comparing these salinity–property plots to a conservative mixing line that assumed the freshwater and marine end-members to be CES01 and SCBM6. The deviation from this conservative mixing line was calculated using the following equation:

$$PercentDeviation(\%) \frac{A_o - A_c}{A_c} \times 100 \qquad (5)$$

where A_c is the area under the conservative mixing line and A_o is the area under the curve defined by the observed CDOM distributions. Percentages less than 0 indicate loss of CDOM during mixing, while positive values suggest addition. Due to inherent uncertainties in measurements of salinity and CDOM, any mixing with percent deviations within ±3 % was considered conservative by trial and error. Selection of a different value would not impact the overall conclusions of this study.

Following McPherson and Miller (1994), the partial attenuation coefficients for color, turbidity, and Chl a to k_d were quantified using multiple stepwise linear regression (SAS 9.3). While optical models may provide a more mechanistic representation of the relationship between light attenuation and water quality concentrations, development of such models requires region-specific relationships between water quality concentrations and inherent optical properties (IOPs) (Gallegos 2001). More importantly, optical models are very sensitive to these relationships, and such relationships are highly variable from region to region. Due to the lack of those relationships for our study region, we chose to apply a commonly used regression model to link light attenuation and water quality.

The regression related k_d to the concentrations of the three water quality parameters measured at a depth of ~0.5 m. In the regression model, a forced intercept of 0.15 was specified. The value of 0.15 is the contribution of pure water to the total light attenuation coefficient at a depth of around 2 m (the depth over which k_d was calculated (Kelly Dixon, Mote Marine Laboratory, personal communication). Presently, there is no known method for calculating the partial R^2 for each of the multiple regression coefficients when the intercept is forced through a specified value (SAS, personal communication). The regression coefficients in the model represent estimates of the partial light attenuation coefficients for each water quality parameter. The relative contribution of each water quality parameter to total light attenuation (k_d) was calculated by dividing the partial light attenuation due to each parameter (product of a regression coefficient and concentration) by total light attenuation (k_d).

Results

Freshwater Inflow at S79

The Caloosahatchee River flows at S79 ranged from 0 to 300 m^3 s^{-1} with an average flow of ~43 m^3 s^{-1} over the sample period and exhibited a distinctive seasonal variability with higher flows (e.g., >43 m^3 s^{-1}) in the wet season (May–October) and lower flows (<43 m^3 s^{-1}) in the dry season (November–April, except April 2010 when the average flow over the 21 days prior to sampling was about 43 m^3 s^{-1}). Our surveys were almost evenly distributed between the two seasons with six cruises in the wet and eight in the dry season based on sampling dates (Fig. 2 and Table 1).

CDOM Distribution and Variation in the CRE

CDOM in the CRE showed considerable variation with $a_{CDOM}(355)$ ranging from 0.5 to 64.0 m^{-1} (corresponding to color of ~1–200 PCU) with an average and standard deviation of 20.0 and 15.0 m^{-1}, respectively. Overall, CDOM showed longitudinal gradients with high concentrations in freshwater (15.0–64.0 m^{-1}) and lower concentrations in the lower estuary and Gulf of Mexico waters (0.5–1.5 m^{-1}), resulting in an inverse relationship with salinity (Fig. 3a and Table 1).

Variation of CDOM (a_{CDOM}) at each station appeared to be also related to the freshwater inflow to the estuary. In the freshwater Caloosahatchee River upstream of S79, CDOM increased as discharge increased (Fig. 3b). Similar strong and positive relationships between CDOM and inflow rates were observed at other stations (data not shown here, correlation coefficients ranged from 0.6 to 0.8, $p < 0.05$ in all cases).

CDOM Mixing Behavior in the CRE

Although there was a strong inverse relationship between CDOM and salinity (Fig. 3), salinity–property plots for the individual surveys revealed three distinct apparent mixing patterns within the estuary: conservative (Fig. 4a), addition of CDOM (Fig. 4b), and loss of CDOM (Fig. 4c). Conservative mixing in the estuary was observed in three surveys, addition of CDOM to the estuary was observed in four surveys, and loss of CDOM from the estuary was observed in six surveys (Table 1). Furthermore, the percent deviation from the hypothetical conservative mixing line appeared related to

Fig. 2 Daily mean flow rate ($m^3 s^{-1}$) at S79 (the *solid line*) and mean flows (*dashed line*) from January 2009–January 2011 and averaged daily flows over 21 days prior to sampling dates (*open circles*). The *vertical bars* indicate the sampling dates
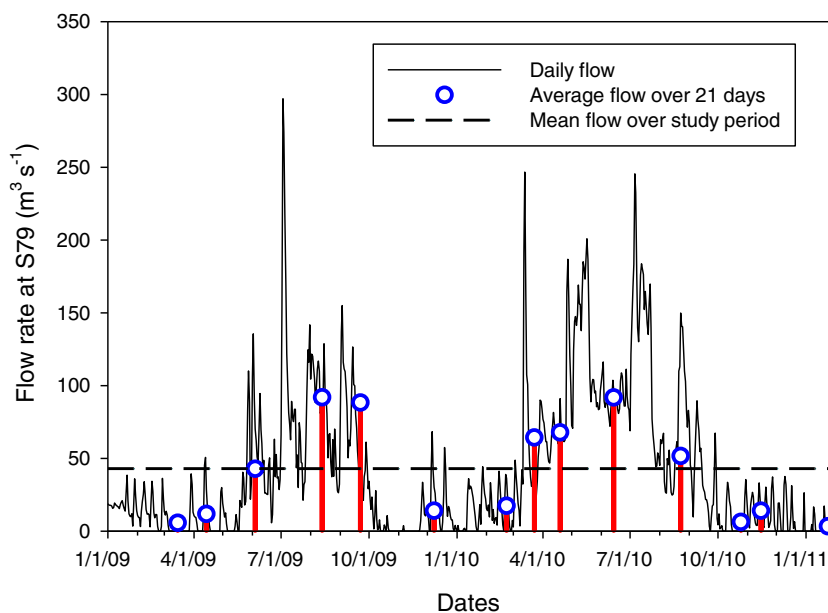
freshwater inflow rates with conservative behavior or addition of CDOM to the estuary at lower flows and loss of CDOM from the estuary at higher flows (Fig. 5). This deviation is because higher CDOM at higher discharge is still lower than the hypothetical conservative estimate, thus showing apparent "loss" of CDOM during higher discharge. By contrast, decreased CDOM at lower discharge is still higher than the estimate from mixing, showing apparent "addition" of CDOM.

Laboratory Experiments

While apparent mixing in the field exhibited three different patterns, all dilution experiments showed conservative mixing between river and ocean end-members (see the three examples in Fig. 4), suggesting that flocculation was not a major loss process of CDOM during mixing. By contrast, during the photolysis experiments, the concentration of CDOM (as measured by the absorption coefficient at 355 nm) decreased exponentially as a function of cumulative PAR exposure, while no loss was observed in all dark control samples (Fig. 6). This photochemical degradation was observed in all photolysis experiments with estimated photolysis rates (k_p) ranging from 0.002 to 0.004 $m^2 mol^{-1}$ (Table 1). Furthermore, the spectral ratio, S_R, increased with time over the course of the photolysis experiments (Fig. 7a). This increase was more pronounced when the S_R was normalized to the initial values measured on day 0 (Fig. 7b).

Partitioning of the Light Attenuation Coefficient

The light attenuation coefficient, k_d, varied from 0.53 to 3.65 m^{-1} with an average and standard deviation of 1.5 and

0.69 m^{-1}, respectively. Together, color (CDOM), turbidity, and Chl a explained 96 % of the variation in k_d (eq 6). The regression coefficients were all significantly greater than 0 ($p < 0.01$).

$$K_d = 0.15 + 0.020 \times color + 0.069 \times turbidity + 0.032 \quad (6)$$
$$\times Chl\, a (n = 52, r^2 = 0.96, p < 0.001)$$

Using these coefficients and concentrations of color, turbidity, and Chl a observed in the field, we estimated the relative contribution of color, turbidity, and Chl a to predicted k_d at each station from the last four cruises (Table 2). The contribution of CDOM to k_d ranged from more than 90 % in the upper estuary to <5 % in the lower estuary with an average of 55 %. By contrast, the contribution of turbidity to k_d varied from <5 % in the upper estuary to 79 % in the lower estuary with an average of 23 %. Chl a accounted for 2–24 % of the total light attenuation with an average of 12 % and showed no apparent spatial pattern.

Discussion

CDOM Distribution

The CDOM absorption coefficient at 355 nm ($a_{CDOM}(355)$, m^{-1}) varied from 0.5 to 64.0 m^{-1} in this study with 15.0–64.0 m^{-1} in the upper estuary and 0.5–1.5 m^{-1} in San Carlos Bay and the Gulf of Mexico in the lower estuary. These ranges are consistent with those commonly observed in oceanic waters (0.5–1.0 m^{-1}) (Rochelle-Newall and Fisher 2002) and those in other subtropical estuaries in southern Florida.

Fig. 3 a Relationship between CDOM absorption coefficient (m^{-1}) at 355 nm and salinity. **b** Relationship between CDOM absorption coefficient (m^{-1}) at 355 nm or color (PCU) collected from station CES01 and flow rates at S79 averaged over 21 days prior to the sample dates. The overlaid lines are linearly fitted curves
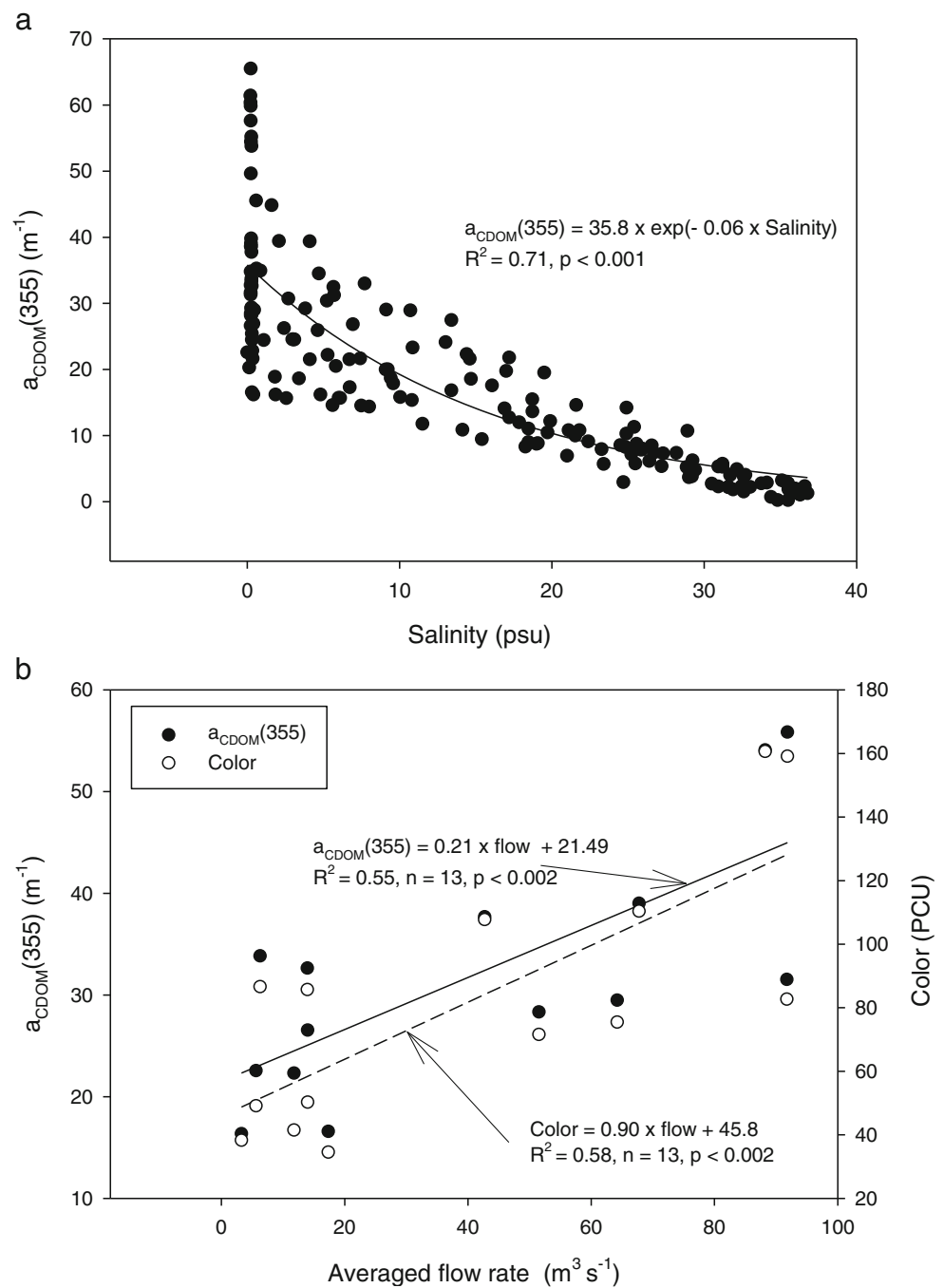

Gallegos (2005) found that the CDOM absorption coefficient at 400 nm in the St. Johns River ranged from 14 to 30 m^{-1}, corresponding to 30–60 m^{-1} at 355 nm if a CDOM spectral slope of 0.015 nm^{-1} is assumed (Kirk 1994). Similarly, Chen et al. (2007) found that CDOM in Tampa Bay, Florida, varied from 10 to 50 m^{-1} when converted to the absorption coefficient at a wavelength of 355 nm from reported values at 400 nm using the same slope of 0.015 nm^{-1}. However, these values are much higher (up to one order of magnitude) than CDOM from some larger water bodies such as the Mississippi River (2.0 m^{-1} at 412 nm or ~5.0 m^{-1} at 355 nm, Del Castillo and Miller 2008) and the Chesapeake Bay (2–5 m^{-1} at 355 nm, Rochelle-Newall and Fisher 2002).

The concentration of CDOM decreased as salinity increased with distance downstream of S79. This observation is consistent with previous studies of the Caloosahatchee (McPherson et al. 1990; Doering and Chamberlain 1999) and is due to mixing of highly colored freshwater with seawater having a relatively lower concentration of CDOM (Fig. 3a). In addition, consistent with previous observations, the concentration of CDOM increased with increasing discharge at S79 (Fig. 3b) (Doering and Chamberlain 1999).

Fig. 4 Examples of three
different mixing behaviors: **a**
conservative mixing, **b** addition,
and (**c**) loss of CDOM in the field
(*filled circles*) and in flocculation
experiments (*open circles*)
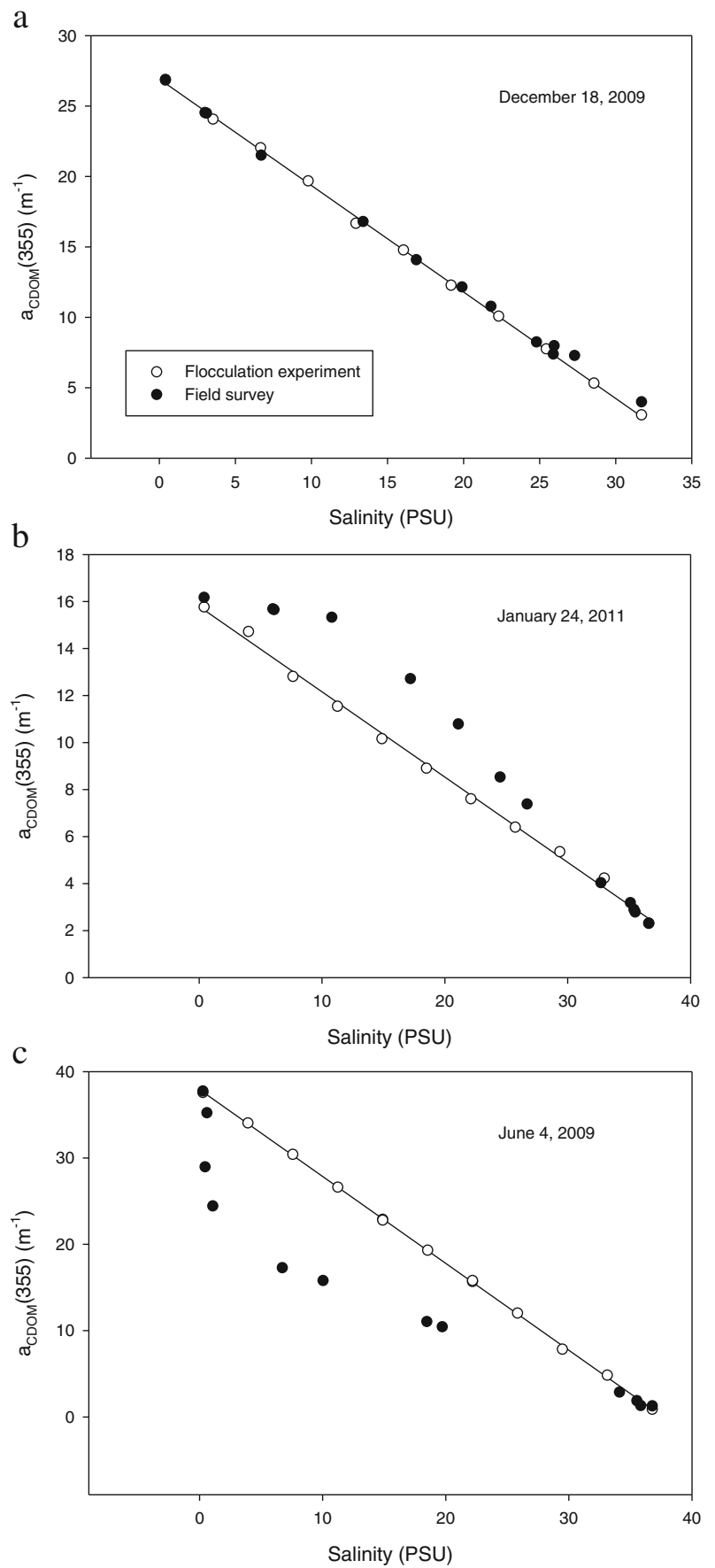
Fig. 5 The relationship between percent deviation from conservative mixing and daily average flow rate at S79 over 21 days prior to sampling


Percentage = -14.6 x ln(flow) + 39.7
$R^2 = 0.67$, n = 13, p < 0.001
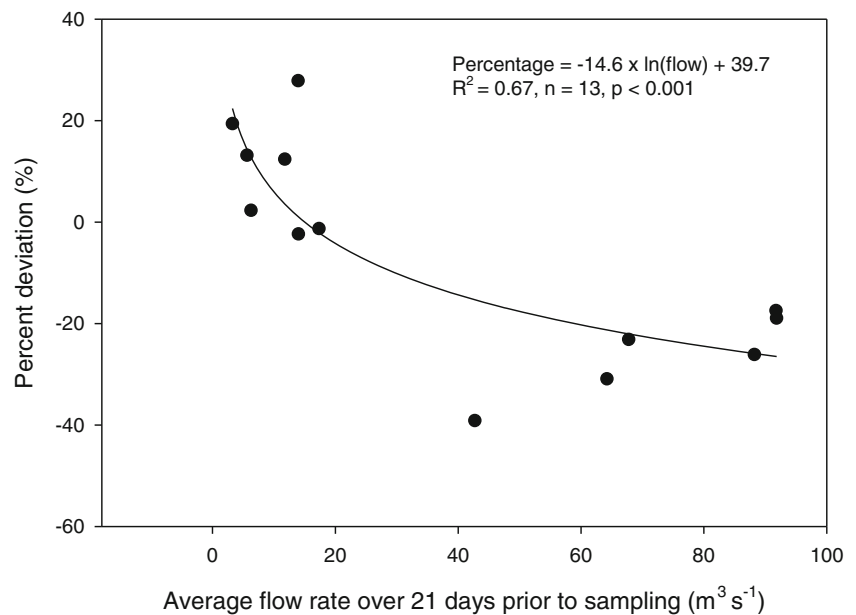
Mixing Behavior

In general, CDOM is thought to behave conservatively in estuaries (Rochelle-Newall and Fisher 2002; Kowalczuk et al. 2003; Chen et al. 2007; Del Castillo and Miller 2008). This expectation is based on observations of higher concentrations of CDOM in freshwater relative to seawater and the assumption that mixing dominates over other processes affecting concentration such as biological release and photochemical reactions.

However, apparent loss of CDOM was observed in the CRE in this study during high freshwater inflows.

Laboratory studies indicated that flocculation was not a major loss in the CRE, although other studies have suggested that flocculation and absorptive removal by sediment could be a major loss of CDOM in humic-rich estuaries (Uher et al. 2001). The difference may be due to a lower sediment concentration in the CRE where average total suspended solid (TSS) concentration is ~15 mg L^{-1} as compared to sediment concentration required for the observable loss of CDOM due to sediment absorption reported by Uher et al. (2001) where average sediment concentrations were 100–1000 mg L^{-1}. Indeed, Shank et al. (2005) estimated that only 1 % of CDOM can

Fig. 6 An example of the relationship between CDOM absorption coefficient at 355 nm ($a_{CDOM}(355)$, m^{-1}) and the cumulative exposure to PAR (PAR$_{cum}$, mol m^{-2}) during a photolysis experiment conducted in June 2010. Experimental flasks exposed to light (*filled circle*) and dark control (*open circle*) flasks

June 2010

$a_{CDOM}(355) = 29.6 \times e^{-0.0025 \times PAR}$

$R^2 = 0.98$, N = 5, p < 0.001

● Photolysis
○ Dark control
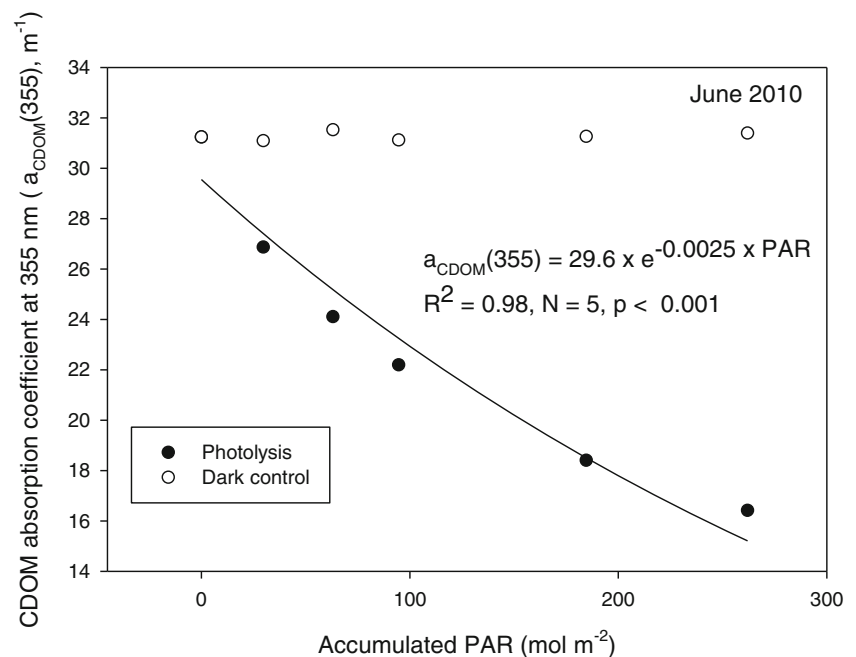
Fig. 7 **a** Absolute changes of ratios of spectral slope (S_R) at 275–295 nm to slope at 350–400 nm and **b** percent changes in S_R relative to initial S_R with irradiation time (days)
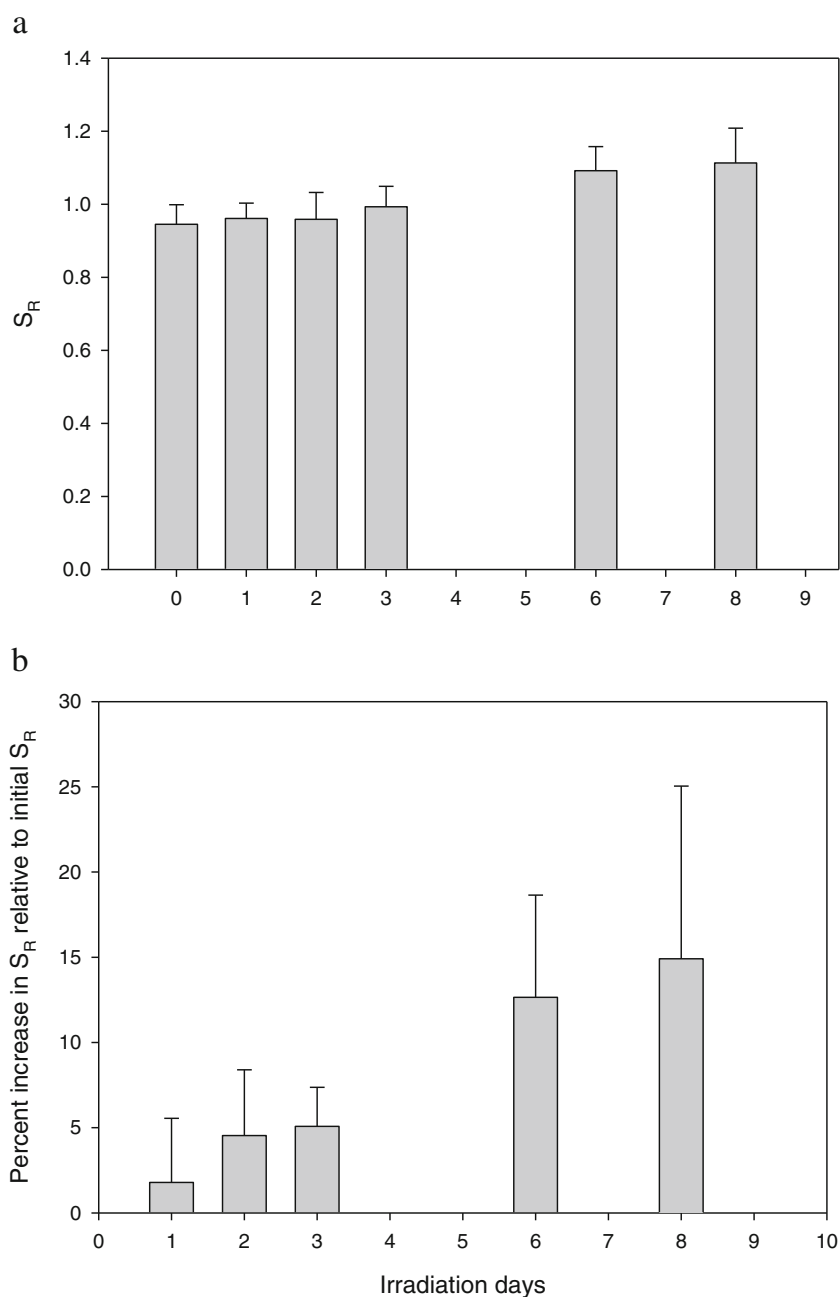
be removed at suspended sediment concentration of 10–20 mg L^{-1}. Similarly, negligible effects of flocculation on CDOM were observed in other rivers with low suspended sediment concentration (Del Castillo et al. 2000).

Laboratory experiments demonstrated that CDOM from the Caloosahatchee was consistently susceptible to photolysis based on decreases in concentration and increases in spectral ratios upon exposure to natural sunlight, similar to the findings of Helms et al. (2008). Previous studies also suggested that CDOM is susceptible to photolysis in estuarine and coastal waters (Chen et al. 2007; D'Sa and DiMarco 2009; Shank et al. 2009). The

estimated decay rates ($\sim$0.003 m^2 mol^{-1}) imply a half-life (reduction to 50 % initial concentration) of CDOM in the CRE due to photolysis of approximately 1 week (0.53= exp ($-$0.003 m^{-1} mol^{-1}×30 mol m^{-2} day^{-1}×7 day)) assuming an annual mean PAR of $\sim$30 mol m^{-2} day^{-1} (ranging from 23 to 45 mol m^{-2} day^{-1}) for the CRE area (unpublished data). This half-life of CDOM is a simplified estimate because attenuation of PAR through the water column was not considered, but the value is similar to the CDOM bleaching rates reported in other subtropical estuarine systems (Shank et al. 2009). Thus, photolysis is at least partly responsible for the observed CDOM loss

Table 2 Percent contributions (average (minimum–maximum)) of color, Chl *a* and turbidity to total light attenuation at each station

| Stations	Color	Chl a	Turbidity
4 CES01	77 (57–91)	11 (2–19)	8 (3–15)
Marker 2	83 (65–91)	5 (3–10)	8 (3–14)
Marker 6	76 (57–92)	13 (2–24)	6 (5–10)
Marker 27	76 (46–89)	8 (3–16)	12 (6–29)
Marker 52	71 (46–82)	10 (5–16)	14 (7–29)
Marker 66	65 (46–73)	14 (13–21)	13 (4–23)
Marker 74	60 (51–67)	12 (12–13)	18 (13–21)
Marker 83	54 (27–66)	9 (6–12)	27 (3–55)
Shell Point 50	(37–57)	9 (6–15)	24 (9–33)
Marker 101	33 (17–49)	13 (8–16)	38 (21–52)
South 6	29 (2–58)	9 (7–12)	48 (16–79)
Green 11	24 (3–45)	14 (8–18)	44 (20–60)
SCB Marker 6	24 (3–45)	12 (11–16)	42 (16–67)

during periods of high freshwater inflow. More importantly, photolysis does not only directly decrease CDOM concentration but also it stimulates bacterial activity and thus enhances microbial degradation of CDOM because of production of biologically labile products (Miller and Moran 1997; Shank et al. 2009). The photochemical and microbial decomposition of CDOM is likely at the highest level during the period of high freshwater inflow because of coincident high temperature and ample solar irradiation during the wet season. Thus, based on the consistently observed photolysis in the laboratory experiment and its

potentially enhanced microbial degradation of CDOM, it is expected that more appreciable CDOM could be lost during the period of high freshwater inflow.

CDOM also showed apparent addition in the CRE when freshwater inflows were relatively lower. Previous studies also found similar results in estuarine and coastal waters (Doering et al. 1994; Rochelle-Newall and Fisher 2002). This additional CDOM relative to conservative mixing is likely due to sources other than inputs from S79. CDOM inputs from other tributaries in the watershed likely contribute to this increase, and their contributions become significant when CDOM input from S79 is relatively small. In addition, CDOM can be produced in situ by phytoplankton (Romera-Castillo et al. 2010), mangroves, sea grass (Shank et al. 2010), and from resuspension of bottom sediments (Boss et al. 2001). Further investigation is needed to clearly identify additional sources of CDOM in the CRE.

It should be noted that the assessment of the mixing behavior of CDOM in the CRE is based on analysis of salinity–property plots. This approach assumes that the concentrations of two end-members vary on a time scale comparable to the estuarine flushing time. When this assumption is invalid, the resulting conservative mixing line is not linear (Officer and Lynch 1981; Cifuentes et al. 1990; Bowers and Brett 2008). We cannot fully evaluate the effects of end-member CDOM fluctuation and variable flushing time due to the lack of high frequency CDOM measurements in the CRE. However, the consistent variation of CDOM mixing behavior from low to high freshwater discharge (Fig. 5) suggests that errors introduced by the assumptions are relatively small.

Fig. 8 Effect of nonconservative mixing of CDOM on the diffuse light attenuation coefficient (k_d) in the Caloosahatchee Estuary and San Carlos Bay. *Y*-axis is the percent deviation of observed k_d from that calculated using a regression model and assuming a concentration based on conservative mixing of CDOM. Data for four cruises are presented
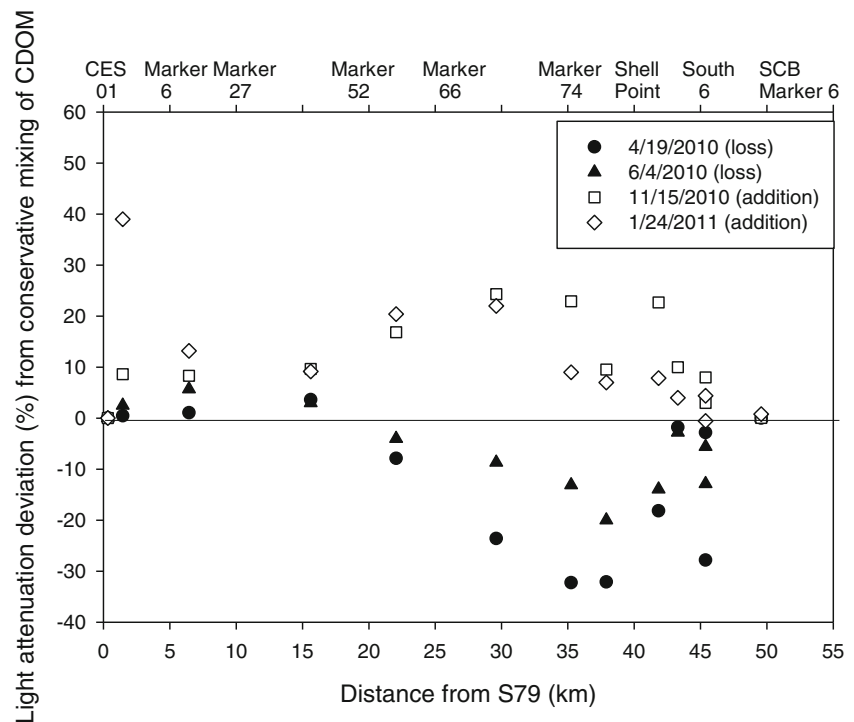
Light Availability

Our study found light attenuation to be primarily controlled by CDOM in the upper Caloosahatchee Estuary and by turbidity in the more marine San Carlos Bay (Table 2). Including all data, CDOM accounted for an average of 55 % of the light attenuation, with turbidity and Chl a contributing 23 and 12 %, respectively. At all stations, Chl a contributed the least to light attenuation relative to CDOM or turbidity. This low contribution of Chl a to the total light attenuation is consistent with previous results in the CRE (McPherson and Miller 1994; Dixon and J. Kirkpatrick 1999) and other subtropical estuaries (Christian and Sheng 2003; Kelble et al. 2005). However, the relatively low contribution of Chl a to light attenuation in the CRE is different from observations in and other large estuaries (e.g., Chesapeake Bay) and even other south Florida estuaries (e.g., Tampa Bay), where k_d was dominated by the variability of phytoplankton and sediment (Gallegos 2001; Le et al. 2013). The differences are mostly due to the higher CDOM concentration in the CRE.

The relative contributions of the three constituents are based on a regression model with a forced intercept of 0.15, which represents the attenuation due to water at a depth of 2 m. An alternative approach is to allow the intercept to be calculated along with the other regression coefficients. With this approach, color (CDOM), turbidity, and Chl a explain ~87 % (slightly smaller than that using a forced intercept) of the variation in k_d with partial R^2 of color, turbidity, and Chl a of 0.84, 0.018, and 0.007, respectively. This approach also results in a larger intercept (0.48 vs. 0.15) and smaller regression coefficients for turbidity (0.038 vs. 0.069) and Chl a (0.015 vs. 0.032), and virtually equal coefficient for color (0.018 vs. 0.019). McPherson and Miller (1994) used this method and derived an intercept of 0.30. Thus, using this approach of unforced intercept does not change the general conclusions: Light attenuation in the CRE is primarily controlled by CDOM (average over all stations =50 vs. 55 %), followed by turbidity (average over all stations =18 vs. 23 %) with chlorophyll a (average overall stations =8 vs. 12 %) contributing the least.

Previous studies have demonstrated the importance of light attenuation in controlling the productivity of phytoplankton and benthic microalgae and the depth distribution of sea grasses in the Caloosahatchee Estuary and San Carlos Bay (McPherson et al. 1990; Dixon and Kirkpatrick 1999; Corbett and Hale 2006). Our study indicates that the apparent mixing behavior of CDOM in the estuarine region of the study area can increase or decrease light attenuation by up to 30 % (Fig. 8). This can have serious ecological consequences for sea grasses in the CRE. Sea grass subsurface light requirements of about 25 % of surface irradiance (Corbett and Hale 2006) dictate the critical depth of sea grass, below which sea grass will not survive. Changes in the light attenuation will

also cause changes to this critical depth. For example, during our study, the mean k_d at Marker 66 during low flow conditions, when addition of CDOM occurred, was about 1.6 m^{-1}, implying a critical depth of 0.86 m. Assuming conservative mixing under low flow conditions (i.e., addition of CDOM did not occur) would result in a 30 % decrease in light attenuation (Fig. 8), yielding a k_d of about 1.2 m^{-1} and a deeper critical depth of about 1.15 m.

The contribution of Chl a to light attenuation when compared to CDOM and turbidity in the Caloosahatchee and San Carlos Bay has additional management implications. Sea grass management strategies designed to improve water clarity and light penetration by lowering Chl a concentrations through nutrient load reduction have been successful in systems like Tampa Bay where Chl a is a major attenuator of light (Le et al. 2013; Greening et al. 2011). In systems like the Caloosahatchee where CDOM and turbidity dominate light attenuation, the success of such an approach is less assured. Indeed, sea grass modeling results demonstrated a similar system where light is controlled primarily by CDOM and turbidity, and sea grass growth is not very sensitive to changes in Chl a (Buzzelli et al. 2012). Even in Tampa Bay, the beneficial effects of nutrient load reduction on sea grass restoration have been more muted than expected in some areas due to the contribution of turbidity and CDOM to light attenuation (Greening et al. 2011).

References

Boss, E., W.S. Pegau, J.R.V. Zaneveld, and A.H. Barnard. 2001. Spatial and temporal variability of absorption by dissolved material at a continental shelf. *Journal of Geophysical Research* 106: 9499–9507.

Blough, N.V., and R. Del Vecchio. 2002. Chromophoric DOM in the coastal environment. P509-546. In D.A. Hansell and C.A. Carlson [eds.]. Biogeochemistry of marine dissolved organic matter. Academic Press.

Bowers, D.G., and H.L. Brett. 2008. The relationship between CDOM and salinity in estuaries: An analytical and graphic solution. *Journal of Marine Systems* 73: 1–7.

Branco, A.B..., and J.N. Kremer. 2005. The relative importance of chlorophyll and colored dissolved organic matter (CDOM) to the prediction of the diffuse attenuation coefficient in shallow estuaries. *Estuaries* 28: 643–652.

Buzzelli, C., R. Robbins, P.H. Doering, Z. Chen, D. Sun, Y. Wan, B. Welch, and A. Schwarzchild. 2012. Monitoring and modeling of Syringodium filiforme (Manatee Grass) in the southern Indian River Lagoon. *Estuaries and Coasts* 35: 1401–1415.

Chen, Z., C. Hu, R.N. Conmy, F. Muller-Karger, and P. Swarzenski. 2007. Colored dissolved organic matter in Tampa Bay, Florida. *Marine Chemistry* 104: 98–109.

Christian, D., and Y.P. Sheng. 2003. Relative influence of various water quality parameters on light attenuation in Indian River Lagoon. *Estuarine, Coastal and Shelf Science* 57: 961–971.

Cifuentes, L.A., L.E. Schemel, and J.H. Sharp. 1990. Qualitative and numerical analyses of the effects of river flow variations on mixing diagrams in estuaries. *Estuarine, Coastal and Shelf Science* 30: 411–427.

Corbett, C.A., and J.A. Hale. 2006. Development of water quality targets for Charlotte Harbor, Florida using seagrass light requirements. *Florida Scientist* 69: 36–50.

Del Castillo, C.E., F. Gilbes, P.G. Coble, and F.E. Muller-Karger. 2000. On the dispersal of riverine colored dissolved organic matter over the West Florida Shelf. *Limnology and Oceanography* 45: 1425–1432.

Del Castillo, C.E., and R.L. Miller. 2008. On the use of ocean color remote sensing to measure the transport of dissolved organic carbon by the Mississippi River plume. *Remote Sense of Environment* 112: 836–844.

Dixon, L., and J. Kirkpatrick. 1999. Causes of light attenuation with respect to seagrasses in Upper and lower Charlotte Harbor. Final Report. Submitted to: Southwest Florida Water Management District, Surface Water Improvement and Management Program. 7601 US Hwy 301 North, Tampa, Florida.

Doering, P.H., C.A. Oviatt, J.H. Mckenna, and L.W. Reed. 1994. Mixing behavior of dissolved organic carbon and its potential biological significance in the Pawcatuck River. *Estuaries* 17: 521–536.

Doering, P.H., and R.H. Chamberlain. 1999. Water quality and source of freshwater discharge to the Caloosahatchee Estuary, Florida. *Journal of the American Water Resources Association* 35: 793–806.

Doering, P.H., R.H. Chamberlain, and K.M. Haunert. 2006. Chlorophyll *a* and its use as an indicator of eutrophication in the Caloosahatchee estuary, Florida. *Florida Scientist* 69: 51–72.

D'Sa, E.J., and S.F. DiMarco. 2009. Seasonal variability and controls on chromophoric dissolved organic matter in a large river-dominated coastal margin. *Limnology and Oceanography* 54: 2233–2242.

Gallegos, C.L. 2001. Calculating optical water quality targets to restore and protect submersed aquatic vegetation: Overcoming problems in partitioning the diffuse attenuation coefficient for photosynthetically active radiation. *Estuaries* 24: 381–397.

Gallegos, C.L. 2005. Optical water quality of a blackwater river estuary: The Lower St. Johns River, Florida, USA. *Estuarine. Coastal and Shelf Science* 63: 57–72.

Greening, H., and A. Janicki. 2006. Toward reversal of eutrophic conditions in a subtropical estuary: Water quality and seagrass response to nitrogen loading reductions in Tampa Bay, Florida USA. *Environmental Management* 38: 163–178.

Greening, H.S., L.M. Cross, and E.T. Sherwood. 2011. A multiscale approach to seagrass recovery in Tampa Bay, Florida. *Ecological Restoration* 29: 82–93.

Helms, J.R., A. Stubbins, J.D. Ritchie, E.C. Minor, D.J. Kieber, and K. Mopper. 2008. Absorption spectral slopes and slope ratios as indicators of molecular weight, source, and photobleaching of chromophoric dissolved organic matter. *Limnology and Oceanography* 53: 955–969.

Kelble, C., P.B. Ortner, G.L. Hitchcock, and J.N. Boyer. 2005. Attenuation of photosynthetically available radiation (PAR) in Florida Bay: Potential for light limitation of primary producers. *Estuaries* 28: 560–571.

Kirk, J.T.O. 1994. *2nd Edition, Light and photosynthesis in aquatic ecosystems*. New York, NY: Cambridge University Press.

Kowalczuk, P., W.J. Cooper, R.F. Whitehead, M.J. Durako, and W. Sheldon. 2003. Characterization of CDOM in an organic rich river and surrounding coastal ocean in the South Atlantic Bight. *Aquatic Sciences* 65: 381–398.

Le, C., C. Hu, D. English, J. Cannizzaro, Z. Chen, C. Kovach, C.J. Anastasiou, J. Zhao, and K.L. Carder. 2013. Inherent and apparent optical porperties of the complex estuarine waters of Tampa Bay: What controls light? *Estuarine, Coastal and Shelf Science* 117: 54–69.

McPherson, B.F., and R.L. Miller. 1987. The vertical attenuation of light in Charlotte Harbor, a shallow, subtropical estuary, southwestern Florida. *Estuarine Coastal Shelf Science* 25: 721–737.

McPherson, B.F., R.T. Montgomery, and E.E. Emmons. 1990. Phytoplankton productivity and biomass in the Charlotte Harbor Estuarine system, Florida. *Water Resources Bulletin* 26: 787–799.

McPherson, B.F., and R.L. Miller. 1994. Causes of light attenuation in Tampa Bay and Charlotte Harbor, Southwestern Florida. *Water Resources Bulletin* 30: 43–53.

Miller, W.L., and M.A. Moran. 1997. Interaction of photochemical and microbial processes in the degradation of refractory dissolved organic matter from a coastal marine environment. *Limnology and Oceanography* 42: 1317–1324.

Moran, M.A., W.M. Sheldon, and R.G. Zepp. 2000. Carbon loss and optical property changes during long-term photochemical and biological degradation of estuarine dissolved organic matter. *Limnology and Oceanography* 45: 1254–1264.

Officer, C.B., and D.R. Lynch. 1981. Dynamics of mixing in estuaries. *Estuarine, Coastal and Shelf Science* 12: 525–533.

Ortega-Retuerta, E., T.K. Frazer, C.M. Duarte, S. Ruiz-Halpern, A. Tovar-Sanchez, J.M. Arrieta, and I. Reche. 2009. Biogeneration of chromophoric dissolved organic matter by bacteria and krill in the Southern Ocean. *Limnology and Oceanography* 54: 1941–1950.

Rochelle-Newall, E.J., and T.R. Fisher. 2002. Chromophoric dissolved organic matter and dissolved organic carbon in Chesapeake Bay. *Remote Sensing of Environment* 112: 836–844.

Romera-Castillo, C.H., X.A. Sarmento, B. lvarez-Salgado, J.M. Gasol, and C. Marras. 2010. Production of chromophoric dissolved organic matter by marine phytoplankton. *Limnology and Oceanography* 55: 446–454.

Shank, G.C., R.G. Zepp, R.F. Whitehead, and M.A. Moran. 2005. Variations in the spectral properties of freshwater and estuarine CDOM caused by partitioning onto river and estuarine sediments. *Estuarine, Coastal and Shelf Science* 65: 289–301.

Shank, G.C., K.K. Nelson, and P.A. Montagna. 2009. Importance of CDOM distribution and photoreactivity in a shallow Texas estuary. *Estuaries and Coasts* 32: 661–677.

Shank, G.C., R. Lee, A. Vähätalo, R.G. Zepp, and E. Bartels. 2010. Production of chromophoric dissolved organic matter from mangrove leaf litter and floating *Sargassum* colonies. *Marine Chemistry* 119: 172–181.

South Florida Water Management District (SFWMD). 2013. *SOP LAB-3140, "Standard operating procedure for the determination of chlorophyll-a by fluorescence", version 4*. West Palm Beach: Analytical Services Section.

Uher, G., C. Hughes, G. Henry, and R.C. Upstill-Goddard. 2001. Non-conservative mixing behavior of colored dissolved organic matter in a humic-rich, turbid estuary. *Geophysical Research Letters* 28: 3309–3312.

Wan, Y., C. Qui, P. Doering, M. Ashton, D. Sun, and T. Coley. 2013. Modeling residence time with a three-dimensional hydrodynamic model: Linkage with chlorophyll a in a subtropical estuary. *Ecological Modelling* 268: 93–102.